Genome-wide identification, characterization and expression analysis of the monovalent cation-proton antiporter superfamily, and their function analysis in maize salt tolerance.

Mengsi Kong[1,2†], Meijie Luo[2†], Zhen Feng[2,3], Yunxia Zhang[2], Wei Song[2], Jingna Li[2], Ruyang Zhang[2], Ronghuan Wang[2], Yuandong Wang[2], Jiuran Zhao[2], Yanxin Zhao[2*], Yongsheng Tao[1*].

[1] College of Agronomy, Hebei Agricultural University, Baoding 071001, Hebei, China.

[2] Beijing Key Laboratory of Maize DNA Fingerprinting and Molecular Breeding, Maize Research Center, Beijing Academy of Agriculture and Forestry Sciences (BAAFS), Beijing 100079, China.

[3] Plant Science and Technology College, Beijing University of Agriculture, Beijing 102206, China.

[†] Mengsi Kong and Meijie Luo contributed equally to this work.

* Correspondence: rentlang2003@163.com (Yanxin Zhao); yshtao@126.com (Yongsheng Tao)

Abstract

Background: Sodium toxicity and potassium insufficient are important factors affecting the growth and development of maize in saline soil. The monovalent cation proton antiporter (CPA) superfamily comprises Na^+/H^+ exchanger (NHX), K^+ efflux antiporter (KEA), and cation/H^+ exchanger (CHX) subfamily proteins, which play vital functions in maize salt tolerance.

Results: A total of 35 *ZmCPA* genes were identified in maize, and they were phylogenetically classified into 13 *ZmNHXs*, 16 *ZmCHXs* and 6 *ZmKEAs*. *ZmCPA* genes have a conserved gene structure, with the determined introns range from 11 to 25, 0 to 5 and 16 to 19 in *ZmNHXs*, *ZmCHXs*, *ZmKEAs*, respectively. All proteins have transmembrane domains, with an average transmembrane number of 8, 10, and 10 in ZmNHX, ZmCHX *and* ZmKEA proteins, respectively. Transient expression in maize protoplasts showed that ZmCHX16 and ZmNHX8 are located in the cell membrane. All *ZmCHX* subfamily genes showed lower expression compared to *ZmNHX* and *ZmKEA* subfamilies. Diverse expression in the 60 tissues and modulated expression in response to salt stress suggested *ZmCPAs'* role in maize development and salt stress. Yeast complementary experiment revealed the function of *ZmNHX8*, *ZmCHX8*, *-12*, *-14*, *-16* and *ZmKEA6* in salt tolerance. Maize mutants *zmnhx8* and *zmkea6* further validated the important function of *ZmNHX8* and *ZmKEA6* in salt tolerance. Phosphorylation sites and *cis*-acting regulation elements analyses indicated that phosphorylation and transcriptional regulation may be involved in salt tolerance of *ZmCPA* genes.

Conclusions: Our study provides comprehensive information about *ZmCPA* gene superfamily, which would be useful in their future functional characterization.

Keywords: CPA, maize, Salinity, *ZmNHX*, *ZmCHX*, *ZmKEA*

Background

High salinity stress is a major abiotic stress affecting crop production worldwide. High concentration of salt can reduce the osmotic potential of soil solution and affect the absorption of water by plant roots, resulting in slow growth of new roots and shoots. Meanwhile, Na^+ and Cl^- are absorbed and accumulated to toxic concentrations in plants, which causes the generation of reactive oxygen species (ROS) leading to oxidative stress [1, 2] and senescence of older leaves [3, 4]. To date, many ion channels and transporters have been shown to play crucial roles in maintaining the ion and pH homeostasis in plants under high salinity [5-9]. Among them, the cation transporters have been well characterized and most Na^+ and K^+/H^+ exchangers belong to the monovalent cation/proton antiporter (CPA) superfamily, which is classified into the CPA1 and CPA2 families, according to Transporter Classification database (http://www. tcdb.org/) [10, 11]. The CPA1 consists of Na^+/H^+ exchanger (NHX), while CPA2 consists of K^+ efflux antiporter (KEA) and cation/H^+ exchanger (CHX) subfamilies [12, 13].

The CPA1 family is divided into two main groups, including the intracellular proteins and the plasma membrane-bound proteins, according to the subcellular localization [10]. In *Arabidopsis*, six intracellular NHX isoforms *AtNHX1-6* were identified [14], which localized into the plant vacuole and endosomes, while other two deviating members (*AtSOS1*/*AtNHX7* and *AtNHX8*) are localized into the plasma membrane (PM) [15]. The NHXs consist of 9-12 transmembrane domains (TMs) [16] and are reported to be involved in numerous functions including salt tolerance, pH regulation, ion homeostasis, turgor generation, vesicular trafficking, protein processing and flower development. For instance, ectopic expression of *AtNHX1* causes dramatic salt tolerance in *Arabidopsis* [17,18]. Further, *AtNHX1* and *AtNHX2* are associated with K^+ homeostasis, vacuolar pH control, floral development, reproduction, cell turgor, and regulation of stomata [19]. Endosomal *AtNHX5* and *AtNHX6* play key roles in cell proliferation and growth in *Arabidopsis* [20]. Under salt stress, the expression of *AtSOS1* was induced and increase the stability of its

transcripts [21]. The expression of SOS1 is also induced in leaves and roots of durum wheat after H_2O_2 treatment [22]. Ectopic expression of *GmsSOS1* could alleviate salt tolerance in *Arabidopsis* mutant *atsos1-1* [23]. However, *AtNHX8* is Li^+ specific and performs Li^+ detoxification in *Arabidopsis* [24].

The CPA2 type transporters are predicted to have 8-14 transmembrane domains with a Pfam00999 domain for Na^+, K^+/H^+ exchanger [12]. In *Arabidopsis*, there are 6 members of the KEA subfamily and 28 members of the CHX subfamily [25]. *AtKEAs* are closely related to the bacterial K^+ efflux transporter genes *EcKefB* and *EcKefC*, which are involved in the tolerance to toxic metabolites [26]. The *AtKEA* subfamily contains six genes forming two subgroups in the cladogram: *AtKEA1-3* and *AtKEA4-6*. The cellular localization of *AtKEAs* seemed to be diverse in yeast cells, suggesting each member probably has a different function in K^+ homeostasis and osmotic adjustment [27]. *AtKEA1* and *AtKEA2* are localized in the inner envelop membrane of chloroplasts and *AtKEA3* in the thylakoid membrane. Their functions are chloroplast osmoregulation, and ion and pH homeostasis [28, 29]. *AtCHXs* regulate K^+ and pH homeostasis, and function in controlling membrane trafficking, osmoregulation, and pollen growth and development [30, 31]. In the *AtCHX* subfamily with 9-12 TMs, the expression of 18 *AtCHX* genes is either pollen specific or pollen enhanced, and only 6 are highly expressed in vegetative tissues. This indicates that the multiple *CHX* gene plays an important role in the development, survival, and function of the male gametophyte [32]. *AtCHX14* is located in the PM and regulates K^+ redistribution in *Arabidopsis* [33]. *AtCHX21*, *AtCHX23* and *AtCHX24* have role in salt tolerance [34], chloroplast development and pH homeostasis [35], and leaf senescence, respectively [36]. Moreover, *AtCHX21* and *AtCHX23* are also engaged in guidance of pollen tube to the target ovules [31]. *OsCHX14* played an important role in K^+ homeostasis during flowering in rice [37]. *PbrCHX16* of pear also plays significant role in pollen tube growth [38].

In this study, genome-wide identification of *ZmCPA* genes was firstly conducted in maize. The identified proteins were classified into *ZmNHX*, *ZmKEA* and *ZmCHX*

subfamilies, and used for the analysis of various physicochemical properties like molecular weight (MW), isoelectric point (pI), sub-cellular localization, transmembrane (TM), motifs, structure and evolutionary relationship. The protein-encoding genes were analyzed for the occurrence of splice variants, exon-intron structure and intron phase. Phosphorylation sites and cis-acting regulatory elements were analyzed to investigate the relationship between phosphorylation and transcriptional regulation and the salt tolerance of the *ZmCPA* genes. The *ZmCPA* genes were also analyzed for their expression during numerous developmental stages and in the presence of salinity stresses. Further, six *ZmCPA* genes were cloned and used for functional characterization in the presence of salt. Two maize mutants *zmnhx8* and *zmkea6* were obtained, which further verified the important functions of *ZmNHX8* and *ZmKEA6* in salt tolerance.

Results

Genome-wide identification and characterization of the *CPA* superfamily genes in maize

An extensive BLAST search identified a total of 35 ZmCPA superfamily proteins in the genome of maize (Table S1), which were further confirmed through Pfam database (http://pfam.xfam.org/search) search for the existence of signature Na^+/H^+ exchanger (PF00999) domain. These genes were classified into three subfamilies including 13 *ZmNHX*, 16 *ZmCHX* and 6 *ZmKEA* genes based on protein similarity with the earlier reported the *CPA* genes in *Arabidopsis*. The identified *CPA* genes were named *ZmNHX1-ZmNHX13, ZmCHX1-ZmCHX16 and ZmKEA1-ZmKEA6* based on their order on maize chromosomes (Table S1). The *ZmCPA*s were distributed on all chromosomes of maize, with 5, 3, 3, 4, 1, 3, 5, 4, 3 and 4 *ZmCPA* genes on chromosome 1, 2, 3, 4, 5, 6, 7, 8, 9 and 10, respectively (Figure S1). Each *ZmCPA* gene model was validated by analyzing the similarity between the *ZmCPA* genes and their orthologs of relative species, such as *Arabidopsis*, rice, *Sorghum*, *Brachypodium distachyon* and *Setaria italica* and by analyzing cDNA and DNA sequences of each

ZmCPA gene which were obtained using reverse transcription polymerase chain reaction (RT-PCR) assays with the gene-specific primers listed in Table S2, as most of the *ZmCPA* genes had more than one transcript annotated in MaizeGDB database (Table S1 and Figure S2). By cDNA and DNA sequence alignment analysis, we found that 5 *ZmCPA* genes had alternative splicing events, resulting in multiple transcripts for one gene (Figuer S3), and the transcripts with the conerved gene structure similar to that of their orhologs were selected for further analysis. The gene structures of the *ZmCPA* genes were constructed by aligning their genomic sequences with cDNA sequences obtained by RT-PCR (Figure 1). The number of introns determined in *ZmNHXs*, *ZmCHXs*, *ZmKEAs* ranges from 11 to 25, 0 to 5 and 16 to 19, respectively. (Table 1). The majority of introns in each family were in 0 phase. The *ZmCPA* genes from the same subfamily share the conserved gene structure (Figure 1).

The average protein length of ZmNHX, ZmCHX and ZmKEA proteins were 640, 824 and 815 amino acid (aa) residues, respectively. The average molecular wight (MW) of ZmNHX, ZmCHX and ZmKEA proteins were 70.8, 88.4 and 87.4 kDa, respectively. The isoelectric point (pI) value of ZmNHX, ZmCHX and ZmKEA proteins ranged from 5.28 to 9.07, 5.95 to 9.88, and 5.22 to 6.01, respectively (Table 1).

Phylogenetic analysis of maize *CPA* genes

In order to analyze the evolutionary relationships among the identified *ZmCPA* genes, we aligned their protein sequences with 26 OsCPA and 42 AtCPA proteins to constructed the neighbor-joining (NJ) phylogenetic tree . The detailed information of *AtCPA* and *OsCPA* genes was shown in the Table S3. Based on the topology of the phylogenetic tree, the *CPA* gene superfamily in plants can be subdivided into 3 subfamilies, NHX, CHX and KEA subfamilies. NHX and CHX subfamilies can be further divided into groups N1, N2 and N3, and C1, C2, C3 and C4, respectively. KEA subfamily was formed by K1 and K2 groups. (Figure 2). In addition, we performed a phylogenetic analysis only with ZmCPA proteins. As described in Fig. 3,

ZmCPA genes were also divided into three subfamilies of *ZmNHX*, *ZmCHX*, and *ZmKEA* genes, which is consistent with the classification in Fig. 1. (Figure 3). All groups contain the genes from the three species of *Arabidopsis*, rice, and maize, indicating that the homologous genes in each group have similar conservative functions.

Subcellular localization and motif analysis of *ZmCPA* genes

The transmembrane (TM) helices within ZmCPA proteins were predicted in TMHMM Server v. 2.0 (http://www.cbs.dtu.dk/services/TMHMM/). The results showed that all of ZmCPA proteins have transmembrane domains, and different subfamilies have different transmembrane domains (Figure S4). A maximum of 12 TM regions were predicted in ZmNHX2,-8, ZmCHX3,-11,-16 and ZmKEA4. The average occurrence of TM regions was 8, 10 and 10 in ZmNHX, ZmCHX and ZmKEA proteins, respectively (Table S1). In the NHX and CHX subfamilies, the transmembrane domain is mainly located at the C-terminal, while the transmembrane domain of ZmKEAs is mainly located at the N-terminal. But ZmKEA1, -4, -5 have a single transmembrane domain at the C-terminal. Proteins with different transmembrane domains may have different functions.

We performed the transient expression assay to investigate subcellular localization of ZmCHX16 and ZmNHX8 protiens with in maize protoplasts. The ZmNHX8-GFP and ZmCHX16-GFP fusion proteins were co-localized with OsSCMP1-RFP protien which was rice SECRETORY CARRIER MEMBRANE PROTEIN 1 fused with RFP as a membrane protein control in this study [39], suggesting that ZmNHX8 and ZmCHX16 were localized to plasma membrane (Figure 4). The tertiary stuctures of nine ZmCPA proteins were analyzed by the SWISS-MODEL server [40] and the results showed that similar 3D structures existed among the same subfamily (Figure S5).

Known conserved domains of ZmCAP proteins were identified by screening Pfam database (http://pfam.xfam.org/). All proteins contained the Na^+/H^+ exchanger domain

(PF00999), and 3 ZmKEAs and 5 ZmNHXs also contained Trka_N domian and TatD_relatad DNase domain, respectively (Figure S6). Meanwhile, putative motifs of the ZmCPA proteins were mined with the MEME server (http://meme-suite.org/tools/meme). All of 15 motif sequences identified here were listed in Table S4. Generally, ZmNHX proteins contained 5-8 conserved motifs, and motifs 3,7,9,15 was found in most of them. The ZmCHX and ZmKEA proteins had 6-7 and 2-3 conserved motifs, respectively. Motifs 1 and 11 were present most frequently in ZmCHX and ZmKEA proteins (Figure S6). The conserved domains of the ZmCPA proteins corresponded to partial motifs and covers the transmembrane domain (Figure S4, Figure S6). The results revealed that most closely related members in the same subfamily have common motifs, which indicates functional similarity among the ZmCPA proteins.

Phosphorylation modification of ZmCPA proteins was analyzed with GPS 5.0 (http://gps.biocuckoo.cn/online.php). Most phosphorylated sites residues of all ZmCPA proteins are evenly distributed throughout the protein (Figure S7). On average, 20.5, 23 and 18.6 phosphorylated sites were found in each member of the three subfamilies, respectively.

Cis-elements in promoter sequences of _ZmCPA_ genes

The *cis*-acting regulatory elements interacted with specific transcriptional factors (TFs) are essential for gene expression regulation [41]. The *cis*-acting regulatory elements in promoter sequences of the *ZmCPA* genes were predicted in PlantCARE database (http://bioinformatics.psb.ugent.be/webtools/plantcare/html/) (Figure S8). On basis of functions annotations, the identified *cis*-acting elements were divided into light, stress, and hormone responsive responsive categories. In light responsive category, the G-box, Sp1, ARE, GT1-motif, the MRE, ATCT-motif and the GATA-motif were the common elements in all *ZmCPA* genes. The LTR, ARE, GC-motif, MBS and TC-rich repeats were common elements in the stress response category. The hormone responsive category contained CGTCA-motif, ABRE,

AuxRR-core, TGA-element, P-box, GARE-motif, TATC-box, TCA-element and MBSI.

Expression analysis in different tissues and developmental stages

The NimbleGen maize microarray data [42] (ZM37) including 60 tissues representing 11 major organ systems and various developmental stages of the B73 maize inbred line was employed to analyze the expression pattern of the *ZmCPA* genes. The gene expression data of 31 *ZmCPA* genes including 10 *ZmNHXs*, 16 *ZmCHXs* and 5 *ZmKEAs* was used for cluster analysis. As revealed by the heatmap, all *ZmNHX* genes except *ZmNHX6* and *ZmNHX13* were highly expressed in all 60 tissues (Figure 5). *ZmNHX6* had a much higher expression level in anthers and leaf than other 58 tissues, and *ZmNHX13* was low in all 60 tissues. In case of *ZmKEAs*, all genes were highly expressed in all 60 tissues. All *ZmCHX* genes showed low expression compared to *ZmNHX* and *ZmKEA* subfamilies, and *ZmCHX* genes only exhibited high expression in anthers (Figure 5).

To confirm the organ-specific expression of *ZmCPA* genes revealed by the microarray data, semi-quantitative reverse transcription polymerase chain reaction (semiq-RT-PCR) of 9 *ZmCPA* genes was performed with total RNA isolated from the roots, leaves, ears, immature tassel, pollens, anthers, silk and whole seed (20 days after pollinated) of the B73 inbred line, and the primers for semiq-RT-PCR were listed in Table S5. The semiq-RT-PCR analysis showed that the expression of 8 *ZmCPA* genes was consistent with that of microarray (Figure 6). The *ZmNHX4*, *-5* and *-8* showed specific expression in roots and leaves, while *ZmCHX6*, *-14*, *-16* were specifically expressed in pollens and anthers. *ZmKEA1* and *ZmKEA4* were predominately expressed in all tested tissues except seed (20 days after pollinated). The *ZmKEA6* was not included in the microarray data, and it had the same expression pattern as other *ZmKEA* subfamily genes.

Expression analysis of *ZmCPA* genes under salinity stress

In order to understand the expression response of *ZmCPA* genes to salt stress, two gene subfamilies including 4 *ZmNHX*s and 4 *ZmKEA*s were chosen for expression profile analysis by real-time quantitative reverse transcription polymerase chain reaction (qRT-PCR) with the primers listed in Table S6 (Figure 7). This study analyzed the gene expression response at 1h, 2h, 4h, and 24h after salt stress. Under 100 mM KCl stress condition and in root, *ZmKEA4*, *-5*, *-6* and *ZmNHX4*, *-5*, *-11* were downregulated, while other genes were upregulated at first then downregulated. In leaf, all 8 *ZmCPA*s were upregulated. When treated with 100mM NaCl, expression of *ZmKEA1*, *-5* and *ZmNHX4*, *-5*, *-11* were downregulated, and *ZmNHX8* were upregulated after 24h, while that of the other genes did not change much in root. In leaf, *ZmKEA4*, *-6* and *ZmNHX4*, *-8*, *-11* were upregulated, while other genes were downregulated. In conclusion, these results implied that *ZmCPA*s might play a role in salinity stress tolerance through expression regulation.

Functional analysis of *ZmCPA* genes in yeast under salt stress

To test the function of *ZmCPA*s in salt tolerance, the coding sequences of *ZmNHX8*, *ZmCHX8*, *-12*, *-14*, *-16* and *ZmKEA6* were cloned into the yeast expression vector pDR196 with the promoter PMA1 and then vectors were introduced into a *Saccharomyces cerevisiae* mutant strain AXT3K. The strain AXT3K lacks the function of plasma membrane Na^+-ATPases (ScENA1-4), plasma membrane Na^+, K^+/H^+ antiporter ScNHA1, and vacuolar Na^+, K^+/H^+ antiporter ScNHX1 [43]. Therefore, it is sensitive to high Na^+. The transformed yeast was grown on Arg phosphate (AP) medium with different levels of NaCl (Figure 8). AXT3K mutants failed to grow in medium containing 20 mM NaCl. Expression of *ZmNHX8*, *ZmCHX8*, *-12*, *-14*, *-16* and *ZmKEA6* enhanced AXT3K salt tolerance (Figure 8). These results indicate that *ZmCPAs* have the function of salt tolerance.

Functional analysis of *ZmNHX8* and *ZmKEA6* under salt stress

We obtained two maize mutants of *zmnhx8* (EMS4-0a18d8) *and zmkea6*

(EMS4-02c2af) , which were produced by EMS mutagenesis of B73 inbred line, from Maize EMS induced Mutant Database (MEMD) [44]. The *zmnhx8* and *zmkea6* mutants had pre-termination mutation in *ZmNHX8* (*Zm00001d022504*) and *ZmKEA6* gene (*Zm00001d026645*), causing production of truncated proteins (Figure 9). Phenotype of inbred lines B73 and two maize mutants were analyzed after four days of growth under salt stress. Under normal conditions, the growth status of B73 and mutants was not significantly different. However, the seedling length and dry weight of *zmnhx8* mutant under 100 mM KCl condition were significantly lower than B73 without salt treatment ($P<0.05$). Similarly, the seedling length and dry weight of *zmkea6* mutant under 100 mM NaCl treatment were significantly lower than B73 without salt treatment ($P<0.05$) (Figure 9). These results further verified that *ZmNHX8* and *ZmKEA6* are important salt tolerance-related genes.

Discussion

Ion homeostasis is an essential process for the survival of plants [34] A number of cation transporters have been known to play pivotal functions in plant growth, development, nutrition, and signal transduction [25]. Cation/proton antiporters (CPAs) superfamily comprises an important group of proteins, which are responsible for the exchange of monovalent cations in bacteria, fungi, animals and plants [45]. Up to now, the function of a number of the *CPA* genes have been studied in *Arabidopsis* [14, 17, 18, 20], rice [37], wheat [41], Soybean [23], and *Arachis hypogea* [46]. Most of them shown to play crucial roles in maintaining the ion and pH homeostasis in plants under high salinity [47].

In this study, 35 *ZmCPA*s were identified to analyze the function of this gene family in maize. Earlier six NHX genes of maize have been reported in various studies [48, 49], which were probably named on the basis of their sequence similarity to known plant *CPA* genes. To avoid the ambiguity, we performed nomenclature of each *ZmCPA* gene following their order on the chromosomes. Analysis of chromosomal distribution revealed that *ZmCPA*s were evenly distributed on the 10 chromosomes of

maize. Similarly, the *CPA* genes were derived from all chromosomes in wheat [41], and 15 out of 17 chromosomes in pear [38], respectively. Phylogenetic tree was generated using full-length CPA protein sequences of maize, rice and *Arabidopsis*. The homologous proteins were found tightly clustered due to high homology among them. Classification of the CPA superfamily genes into NHX, KEA and CHX subfamilies and their further categorization into various groups such as N1-N3, K1-K2 and C1-C4 has also been previously performed in *Arabidopsis*, pear [13, 38].

The sub-cellular localization predicted of different species was consistent up to some extent. AtNHXs exhibited vacuole, endosome and plasma membrane localization [12]. Majority of ZmNHX proteins were also predicted for similar localization. ZmKEA2 was predicted chloroplast localization, which similar with AtKEA1, AtKEA2 and AtKEA3. Most of the ZmCHX proteins were predicted to be localized in plasma membrane ,which same as reported for AtCHX13 and AtCHX14 [33, 50]. Since, various tools predicted different localizations of different ZmCPA proteins, we chose *ZmNHX8* and *ZmCHX16* for transient expression in maize protoplast cells, and the results proved that they were expressed on the plasma membrane.

The expression pattern of the *ZmCPA* genes from the NimbleGen maize microarray data showed *ZmNHX6* was highly expressed in leaf and anthers, *ZmNHX9* was found to be grain specific, other *ZmNHX* and *ZmKEA* genes exhibited significant expression during multiple developmental stages. However, *ZmCHXs* were specific expression in anthers. Similar expression trend has been reported for the *CPA* genes in other plant species. *AtNHX1* and *AtNHX2* are required for growth and floral development in *Arabidopsis* [19], *AtNHX5-6* are essential for normal growth and development in *Arabidopsis* [20]. *TaNHX2*, *TaNHX5* and *TaNHX8* genes exhibited significant expression during multiple developmental stages, which suggested their crucial role in growth and development. *TaKEA6* and *TaKEA3* group genes were prominently expressed in certain developmental stages of root, leaf, stem and spike, which suggested their function in tissue development [41]. *TaCHX* family genes showed

distinct expression pattern where most of the genes were relatively highly expressed in anthers [41], which similar to maize suggested their role in reproductive organ development. At the same time, specific expression of genes was verified by semi-qRT-PCR. We studied expressions of the *ZmCPA* genes in the control and salinity treatments using qRT-PCR. Four *ZmKEAs* in high concentration of KCl were upregulated with salinity treatment in leaf, but in root, *ZmKEA4*, *-5*, *-6* were downregulated in high K^+. In *Arabidopsis*, *AtKEA1*, *AtKEA3* and *AtKEA4* expression was enhanced significantly under low K^+ stress (1mM KCl), but *AtKEA2*, *-5*, and *-6* were not [27]. The differential expression in response to K^+ stress suggests that *ZmKEA1* involved in K^+ acquisition under K^+ conditions in maize, whereas *ZmKEA4*, *5* and *6* may have different functions. *ZmNHX8* was upregulated in NaCl treatment, but *ZmNHX4*, *-5*, and *-11* were downregulated in root. *NHX7/SOS1* is critical for excluding Na^+ from plant roots [51] and *ZmNHX2* is associated with a major quantitative trait locus (QTL), *qST1*, which confers salt tolerance on maize plants [52, 53]. Upregulated expressions of *ZmNHX8* in our salinity treatment support the idea that their roles in response to salt stress may be conserved in maize.

Six *ZmCPA*s were cloned in the yeast expression vector pDR196 and introduced into a yeast mutant strain AXT3K. They restored AXT3K mutant resistance to Na^+. *ZmNHX8* had been verified again for its role in salt stress. *AtNHX5* and *AtNHX6* recovered tolerance to salt using a yeast expression system [20]. These results suggest that *ZmNHX*s share a common mode of action and are involved Na^+ transport in maize. Nevertheless, neither *AtCHXs* nor *AtKEAs* have been found to improve yeast growth in salt stress [12, 27]. In this study, *ZmCHX8*, *-12*, *-14*, *-16* and *ZmKEA6* recovered tolerance to high Na^+. This found was different from *Arabidopsis*, suggesting that the CHX and KEA subfamilies are also resistant to salt stress in maize. Growth inhibition of maize EMS mutants *zmnhx8* and *zmkea6* under salt stress once again validated their important functions on salt stress tolerance.

Conclusions

In the present study, we performed identification and characterization of *ZmCPA*

superfamily comprising *ZmNHX*, *ZmKEA* and *ZmCHX* subfamily proteins in the genome of maize. Gene and proteins structure analyses suggested conserved nature of evolutionary related molecules in each subfamily, however they significantly differed from the members of other groups. The occurrence of high composition of helices and coils in tertiary structure, and numerous TM regions supported hydrophobic membrane bound nature of these proteins. Diverse occurrence of differential expression in various tissues and under abiotic stress conditions indicated the importance of these genes in growth and development and stress management. The prediction of phosphorylation sites and *cis*-acting regulatory elements indicates that phosphorylation and transcriptional regulation may be related to the salt tolerance of *ZmCPA* genes. Characterization of *ZmNHX8*, *ZmCHX8*, *-12*, *-14*, *-16* and *ZmKEA6* in yeast established their role in monovalent cation homeostasis and abiotic stress tolerance. This study verified the function of *ZmNHX8* and *ZmKEA6* by phenotypic analysis of mutants. The study provided numerous features of *ZmCPA* genes, and extended the opportunities for functional validation of each gene in future studies. Further, these genes will also be useful in future crop improvement programs for stress tolerance.

Materials and methods

Identification and bioinformatic analysis of *ZmCPA* gene superfamily.

The known *CPA* genes of *Arabidopsis* were used to query the maize AGPv4 gene set (https://download.maizegdb.org/Zm-B73-REFERENCE-GRAMENE-4.0/) using a local BLASTP program with an E-value <1e-10. The putatively identified sequences were further confirmed by HMMER search for the presence of signature Na^+/H^+ exchanger (PF00999) domain.

The phylogenetic tree was constructed using full length CPA protein sequences of maize, *Arabidopsis*, and rice. Alignment of the sequences was done using MUSCLE v3.8.31 program [54], and a phylogenetic tree was built employing neighbor-joining (NJ) method using MEGA 6.0 [55] with the following sets, bootstrap value of 1000,

Poisson model for amino acid substitution model. The transmembrane domains were predicted using the TMHMM Server v. 2.0 (http://www.cbs.dtu.dk/services/TMHMM/). The Predotar [56], TargetP [57] and WoLF PSORT (https://www.genscript.com/wolf-psort.html), three *in silico* programs, were used to predict the putative organellular localization of ZmCPA proteins. All the ZmCPA proteins were modeled using SWISS-MODEL (https://swissmodel.expasy.org/) [40] to simulate their 3D structures. Putative conserved motifs in maize CPA proteins were identified using the MEME Suite 5.1.1 (http://meme-suite.org/tools/meme) with the following sets, motif length of 10-50 aa, maximum number of motifs to find is 15.

Gene structure analysis

The DNA and transcript sequences of *ZmCPA* genes obtained from the maize sequence annotation database MaizeGDB were used to design gene-specific PCR primers with Primer3 (http://primer3.ut.ee/). DNA and cDNA sequences were validated using PCR and RT-PCR with B73 genomic DNA and total RNA as templates and gene-specific primers shown in Table S2. Alignment of validated DNA and cDNA sequences of each maize *CPA* gene was performed to analyze the gene structure of *ZmCPA* genes. Gene structure display server (GSDS 2.0) was used to display the exon-intron structure, and intron phases [58].

Plant materials and treatments

The maize B73 inbred lines was used in this study. For qRT-PCR, the sterilized seeds were plant in a hydroponic equipment described previously [59] with sterile water in a greenhouse at 27/23°C with day/night of 12/12h. Four days later, the plants were incubated in 1× Hoagland solution (PhytoTech, USA) until fully trifoliate leaves. For controls (CK), excessive potassium stress and NaCl stress, maize seedlings were planted in 1× Hoagland solution without treatment, containing 100 mM KCl and containing 100 mM NaCl, respectively. The concentrations were maintained until the

end of the experiments. For RT-PCR analysis, the corresponding genes were detected of CK plants to exclude the effects of plant development.

For maize mutants, the sterilized seeds were cultured hydroponically in a greenhouse at 27/23°C with day/night of 12/12h as above. The 1× Hoagland solution was exchanged every two days. Ten days later, 100 mM KCl and 100 mM NaCl were added. Four days after salt stress, phenotypic analysis was performed.

Expression analysis of *ZmCPA* genes in different tissues.

To investigate the spatiotemporal expression patterns of *ZmCPA* genes, the log2-transformed and RMA-normalized data for *ZmCPA* genes were downloaded from PLEXdb (http://www.plexdb.org/) [60]. A heat map was produced using Lianchuan Bio Cloud Platform (https://www.lc-bio.cn/overview).

RNA isolation and cDNA synthesis

Total RNA was isolated from different tissues of the B73 inbred lines, including seedling roots, leaves, 5-cm ears, immature tassels, anthers, pollens, silks, and seeds of 20 days after pollination, using the Trizol reagent (Invitrogen, USA) according to the manufacturer's protocol. All RNA was purified using the DNase I (Thermo Scientific, China). First-strand cDNA was synthesized from 1μg of total RNA (20 μL reaction volume) using PrimeScript™ 1st Strand cDNA Synthesis Kit (Takara, Japan) according to the manufacturer's protocol.

Semi-quantitative reverse transcription PCR

All gene-specific primers were designed as shown in Table S5. Specific primers for the maize *Actin1* gene (*GRMZM2G126010*) were used as an internal control. Reactions were performed with 2xTaq Master Mix (Vazyme, China) on a Bio-Rad Thermal Cycler (Bio-Rad, USA) using the following procedure: 5 min at 94 °C to start; 33 cycles of 30 s at 94 °C, 30 s at 59 °C and 2 min at 72 °C; and a final extension step of 72 °C for 10 min to complete the reaction, and the *Actin1* transcript

was amplified with 29 PCR cycles. Each PCR pattern was performed in triplicate, mixtures without a template were employed as negative controls, and the maize *Actin1* amplicon served as an internal control for each gene investigated.

Real-time PCR

Real-time PCR was performed using TB Green *Premix Ex Taq*^{TM} II (Takara, Japan). ABI 7500 real-time PCR system (Applied Biosystems, Foster City, CA, USA) was used with the following thermal cycling conditions of 95℃ for 5 min followed by 40 cycles of 95℃ for 15 s, 60℃ for 5 s, and 72℃ for 34 s. The maize *Actin1* gene (*GRMZM2G126010*) was used as an endogenous control to normalize the samples. Based on the cDNA sequences of *ZmCPA* genes, real-time PCR primers (Table S6) were designed with primer 3 (http://primer3.ut.ee/). The experiment was performed with three technical replicates for each sample. The specificity of the PCR reaction was confirmed by melting curve analysis of the amplicons. Comparative $2^{-\Delta\Delta CT}$ method was used to calculate the relative quantities of each transcript in the samples [61].

Prediction of phosphorylation sites and *cis*-regulatory elements

The GPS5.0 (http://gps.biocuckoo.cn/online.php) software was used to predict the phosphorylation site of ZmCPA proteins.The study selected the 2kb sequence in front of the gene coding region (ATG) as the gene's promoter region sequence. Promoter *cis*-regulatory elements were predicted using PlantCARE [62] (http://bioinformatics.psb.ugent.be/webtools/plantcare/html/) and displayed using DOG2.0 [63].

Subcellular localization

The full-length cDNAs of *ZmCHX16* and *ZmNHX8* were amplified using the primers listed in Table S7 and then were introduced into pM999-EGFP vector to construct the

GFP fusion proteins, ZmCHX16-GFP and ZmNHX8-GPF with the ClonExpress II One Step Cloning Kit (Vazyme, China). Constitutive expression of the fused constructs, ZmCHX16-GFP and ZmNHX8-GPF, were driven by the cauliflower mosaic virus 35S promoter. The maize mesophyll protoplasts were isolated and prepared from etiolated leaves according to the established protocols[64]. The plasmids harboring the ZmCHX16-GFP and ZmNHX8-GPF fusion constructs each was co-transfected with the OsSCAMP1-RFP construct into the protoplast cells. OsSCAMP1 is a known rice secretory carrier membrane protein and used here as a membrane protein control [39]. The transformed protoplast cells were cultured at room temperature overnight and were observed using an Leica SP8 confocal microscope (Leica, USA).

Functional expression of *ZmCPAs* in yeast

The coding sequences of *ZmNHX8*, *ZmCHX8*, *ZmCHX12*, *ZmCHX14*, *ZmCHX16*, *ZmKEA6* were cloned into the PDR196 vector, and then transformed into the yeast strain AXT3K (*ena1-4::HIS3,nha1::LEU2, nhx1::KanMX*). The transformed yeast cells were cultured overnight at 29°C in YPDA medium containing 1 mM KCl. Cells were normalized in water to A_{600} of 0.8. For cation tolerance testing, 5μL aliquots from yeast cultures or 10-fold serial dilutions were spotted onto AP [65] plates supplemented with 1 mM KCl with or without NaCl.

Acknowledgements

We thank Prof. Liwen Jiang (Chinese University of Hong Kong) for kindly providing pM999-EGFP and membrane protein marker (OsSCAMP1-RFP) plasmids, Prof. Xiaoduo Lu (Qilu Normal University) for identifying and providing maize EMS mutants *zmkea6* and *zmnhx8*, and Profs. Yi Wang and Zhenxian Zhang (China Agricultural University) for kindly sharing yeast mutant AXT3K and yeast expression vector pDR196.

Authors' contributions

YST, YXZ(Yanxin Zhao) and JRZ conceived the experiment. MSK, YXZ(Yunxia Zhang), ZF, WS, JNL, RYZ, RHW and YDW performed bioinformatic analysis and data acquisition. MSK, MJL, and YXZ(Yanxin Zhao) analyzed the data and wrote the manuscript. All authors revised and approved the final manuscript, and agreed to be accountable for this work.

Funding

This research was financially supported by the Beijing Municipal Natural Science Foundation (6204041), the Construction of Collaborative Innovation Center of Beijing Academy of Agricultural and Forestry Sciences (Collaborative Innovation Center of Crop Phenomics, KJCX201917) and the Beijing Scholars Program (BSP041). The funding body does not play roles in the design of the study and collection, analysis, and interpretation of data and in writing the manuscript.

Availability of data and materials

The datasets and materials used and/or analyzed during the current study are available from the corresponding author on reasonable request.

Ethics declarations

Ethics approval and consent to participate

Not applicable.

Consent for publication

All authors read and approved the final manuscript.

Competing interests

The authors declare that they have no competing interests.

References

1. Zhu JK. Plant salt tolerance. Trends Plant Sci. 2001;6:66–71.
2. Gupta B, Huang B. Mechanism of salinity tolerance in plants: physiological, biochemical, and molecular characterization. Int J Genom. 2014;1:701596.
3. Munns R, Tester M. Mechanisms of salinity tolerance. Annu Rev Plant Biol. 2008;59:651–681.
4. Teakle NL, Tyerman SD. Mechanisms of Cl^- transport contributing to salt tolerance. Plant Cell Environ. 2010;33:566–589.
5. Pardo JM, Cubero B, Leidi EO, Quintero FJ. Alkali cation exchangers: roles in cellular homeostasis and stress tolerance. J Exp Bot. 2006;57:1181–1199.
6. Ward JM, Mäser P, Schroeder JI. Plant ion channels: gene families, physiology, and functional genomics analyses. Annu Rev Physiol. 2009;71(1):59–82.
7. Barbier-Brygoo H, De Angeli A, Filleur S, Frachisse JM, Gambale F, Thomine S, Wege S. Anion channels/transporters in plants: from molecular bases to regulatory networks. Annu Rev Plant Biol. 2011;62(62):25–51.
8. Yamaguchi T, Hamamoto S, Uozumi N. Sodium transport system in plant cells. Front Plant Sci. 2013;4:410.
9. Hamamoto S, Horie T, Hauser F, Deinlein U, Schroeder JI, Uozumi N. HKT transporters mediate salt stress resistance in plants: from structure and function to the field. Curr Opin Biotechnol. 2015;32:113–120.
10. Pires IS, Negrão S, Pentony MM, Abreu IA, Oliveira MM, Purugganan MD. Different evolutionary histories of two cation/proton exchanger gene families in plants. BMC Plant Biol. 2013;13(1): 97.
11. Saier MH, Reddy VS, Tamang DG, Västermark A. The transporter classification database. Nucleic Acids Res. 2014;42(D1):D251–D258.
12. Chanroj S, Wang G, Venema K, Zhang MW, Delwiche CF, Sze H. Conserved and diversified gene families of monovalent Cation/H^+ Antiporters from algae to flowering plants. Front Plant Sci. 2012;3:25.

13. Ye CY, Yang X, Xia X, Yin W. Comparative analysis of cation/proton antiporter superfamily in plants. Gene. 2013;521(2):245–251.
14. Yokoi S, Quintero FJ, Cubero B, Ruiz MT, Bressan RA, Hasegawa PM, Pardo JM. Differential expression and function of *Arabidopsis thaliana* NHX Na^+ /H^+ antiporters in the salt stress response. Plant J. 2002;30(5):529–539.
15. Elias B, Aadian C, Eduardo B. Cellular ion homeostasis: emerging roles of intracellular NHX Na^+/H^+ antiporters in plant growth and development. J Exp Bot. 2012;63(16):5727–5740.
16. Yamaguchi T, Apse MP, Shi H, Blumwald E. Topological analysis of a plant vacuolar Na^+/H^+ antiporter reveals a luminal C terminus that regulates antiporter cation selectivity. Proc Natl Acad Sci USA. 2003;100(21):12510–12515.
17. Apse MP, Aharon GS, Snedden WA, Blumwald E. Salt tolerance conferred by overexpression of a vacuolar Na^+/H^+ antiport in *Arabidopsis*. Science. 1999;285(5231):1256–1258.
18. Apse MP, Sottosanto JB, Blumwald E. Vacuolar cation/H^+ exchange, ion homeostasis, and leaf development are altered in a T-DNA insertional mutant of *AtNHX1*, the *Arabidopsis* vacuolar Na^+/H^+ antiporter. Plant J. 2003;36:229–239.
19. Barragán V, Leidi EO, Andrés Z, Rubio L, De Luca A, Fernández JA, Cubero B, Pardo JM. Ion exchangers NHX1 and NHX2 mediate active potassium uptake into vacuoles to regulate cell turgor and stomatal function in *Arabidopsis*. Plant Cell. 2012;24(3):1127–1142.
20. Bassil E, Ohto M, Esumi T, Tajima H, Zhu Z, Cagnac O, Belmonte M, Peleg Z, Yamaguchi T, Blumwald E. The *Arabidopsis* intracellular Na^+/H^+ antiporters NHX5 and NHX6 are endosome associated and necessary for plant growth and development. Plant Cell. 2011;23(1):224–239.
21. Jiang J, Shi H. Signaling control of *SOS1* mRNA stability. Plant Signal Behav. 2008;3(9):687–688.
22. Feki K, Tounsi S, Masmoudi K, Brini F. The durum wheat plasma membrane Na^+ /H^+ antiporter SOS1 is involved in oxidative stress response. Protoplasma. 2016;254(4):1–10.
23. Nie W, Xu L, Yu B. A putative soybean *GmsSOS1* confers enhanced salt tolerance to transgenic *Arabidopsis sos1-1* mutant. Protoplasma. 2015;252(1):127–134.
24. An R, Chen Q J, Chai M F, Lu P L, Su Z, Qin Z X, Chen J, Wang XC. *AtNHX8*, a member of the monovalent cation: proton antiporter-1 family in *Arabidopsis thaliana*, encodes a putative Li^+/H^+ antiporter, Plant J. 2007;49(4):718–728.
25. Mäser P, Thomine S, Schroeder JI, Ward JM, Hirschi K, Sze H, Talke IN, Amtmann A, Maathuis FJM, Sanders D, Harper JF, Tchieu J, Gribskov M, Persans MW, Salt DE, Kim SA, Guerinot ML. Phylogenetic relationships within cation transporter families of *Arabidopsis*. Plant Physiol. 2001;126(4):1646–1667.
26. Aranda-Sicilia MN, Cagnac O, Chanroj S, Sze H, Rodríguez-Rosales MP, Venema K. *Arabidopsis* KEA2, a homolog of bacterial KefC, encodes a K^+/H^+ antiporter with a chloroplast transit peptide. Biochim Biophys Acta. 2012;1818(9): 2362–2371.
27. Zheng S, Pan T, Fan L, Qiu Q. A novel *AtKEA* gene family, homolog of bacterial K^+/H^+ antiporters, plays potential roles in K+ homeostasis and osmotic adjustment in *Arabidopsis*. PLoS One. 2013;8(11):e81463.
28. Kunz HH, Gierth M, Herdean A, Satoh-Cruz M, Kramer DM, Spetea C, Schroeder JI. Plastidial transporters KEA1, -2, and -3 are essential for chloroplast osmoregulation, integrity, and pH regulation in *Arabidopsis*. Proc Natl Acad Sci USA. 2014;111(20):7480–7485.

29. Aranda-Sicilia MN, Aboukila A, Armbruster U, Cagnac O, Schumann T, Kunz HH, Jahns P, Rodríguez-Rosales MP, Sze H, Venema K. Envelope K^+/H^+ antiporters AtKEA1 and AtKEA2 function in plastid development. Plant Physiol. 2016;172(1):441–449.
30. Chanroj S, Lu Y, Padmanaban S, Nanatani K, Uozumi N, Rao R, Sze H. Plant-specific cation/H^+ exchanger 17 and its homologs are endomembrane K^+ transporters with roles in protein sorting. J Biol Chem. 2011;286(39):33931–33941.
31. Lu Y, Chanroj S, Zulkifli L, Johnson MA, Uozumi N, Chenung A, Sze H. Pollen tubes lacking a pair of K^+ transporters fail to target ovules in *Arabidopsis*. Plant Cell. 2011;23(1):81–93.
32. Sze H, Padmanaban S, Cellier F, Honys D, Cheng NH, Bock KW, Conéjéro G, Li X, Twell D, Ward JM, Hirschi KD. Expression patterns of a novel *AtCHX* gene family highlight potential roles in osmotic adjustment and K^+ homeostasis in pollen development, Plant Physiol. 2004;136(1):2532–2547.
33. Zhao J, Li P, Motes CM, Park S, Hirschi KD, CHX14 is a plasma membrane K-efflux transporter that regulates K^+ redistribution in *Arabidopsis thaliana*. Plant Cell Environ. 2015;38(11):2223–2238.
34. Hall D, Evans AR, Newbury HJ, Pritchard J. Functional analysis of CHX21: a putative sodium transporter in *Arabidopsis*. J Exp Bot. 2006;57(5):1201–1210.
35. Song CP, Guo Y, Qiu Q, Lambert G, Galbraith DW, Jagendorf A, Zhu JK. A probable Na^+ (K^+)/H^+ exchanger on the chloroplast envelope functions in pH homeostasis and chloroplast development in *Arabidopsis thaliana*. Proc Natl Acad Sci USA. 2004;101(27):10211–10216.
36. Hur Y, Kim JH, Lee DJ, Chung KM, Woo HR. Overexpression of *AtCHX24*, a member of the cation/H^+ exchangers, accelerates leaf senescence in *Arabidopsis thaliana*. Plant Sci. 2012;183:175–182.
37. Chen Y, Ma J, Miller AJ, Luo B, Wang M, Zhu Z, Ouwerkerk PBF. OsCHX14 is involved in the K+ homeostasis in rice (*Oryza sativa*) flowers. Plant Cell Physiol. 2016;57(7):1530–1543.
38. Zhou H, Qi K, Liu X, Yin H, Wang P, Chen J, Wu J. Zhang S. Genome-wide identification and comparative analysis of the cation proton antiporters family in pear and four other Rosaceae species. Mol Genet Genomics. 2016;291(4):1727–1742.
39. Lam SK, Siu CL, Hillmer S, Jang S, An G, Robinson DG, Jiang L. Rice SCAMP1 defines clathrin-coated, *trans*-golgi-located tubular-vesicular structures as an early endosome in tobacco BY-2 cells. Plant Cell. 2007;19(1):296–319.
40. Waterhouse A, Bertoni M, Bienert S, Studer G, Tauriello G, Gumienny R, Heer FT, de Beer TAP, Rempfer C, Bordoli L, Lepore R, Schwede T. SWISS-MODEL: homology modelling of protein structures and complexes. Nucleic Acids Res. 2018;46(W1):W296–W303.
41. Sharma H, Taneja M, Upadhyay SK. Identification, characterization and expression profiling of cation-proton antiporter superfamily in *Triticum aestivum* L. and functional analysis of *TaNHX4-B*. Genomics. 2020;112(1):356–370.
42. Sekhon RS, Lin H, Childs KL Hansey CN, Buell CR, de Leon N, Kaeppler SM. Genome-wide atlas of transcription during maize development. Plant J. 2011;66(4):553–563.
43. Quintero FJ, Blatt MR, Pardo JM. Functional conservation between yeast and plant endosomal Na^+/H^+ antiporters. FEBS Lett. 2000;471(2-3):224–228.
44. Lu X, Liu J, Ren W, Yang Q, Chai Z, Chen R, Wang L, Zhao J, Lang Z, Wang H, Fan Y, Zhao

J, Zhang C. Gene-indexed mutations in maize. Mol Plant. 2018;11(3):496–504.

45. Evans AR, Hall D, Pritchard J, Newbury HJ. The roles of the cation transporters CHX21 and CHX23 in the development of *Arabidopsis thaliana*. J Exp Bot. 2012;63(1):59–67.
46. Zhang WW, Meng JJ, Xing JY, Yang S, Guo F, Li XG, Wan SB. The K^+/H^+ antiporter *AhNHX1* improved tobacco tolerance to NaCl stress by enhancing K^+ retention. J Plant Biol. 2017;60(3):259–267.
47. Jia Q, Zheng C, Sun S, Amjad H, Liang K, Lin W. The role of plant cation/proton antiporter gene family in salt tolerance. Biol Plantarum. 2018;62(4):617–629.
48. Zörb C, Noll A, Karl S, Leib K, Yan F, Schubert S. Molecular characterization of Na^+/H^+ antiporters (ZmNHX) of maize (*Zea mays* L.) and their expression under salt stress. J Plant Physiol. 2005;162(1):55–66.
49. Pitann B, Mohamed AK, Neubert AB, Schubert S. Tonoplast Na^+/H^+ antiporters of newly developed maize (*Zea mays*) hybrids contribute to salt resistance during the second phase of salt stress. J Plant Nutr Soil Sci. 2013;176(2):148–156.
50. Zhao J, Cheng NH, Motes CM, Blancaflor EB, Moore M, Gonzales N, Padmanaban S, Sze H, Ward JM, Hirschi KD. AtCHX13 is a plasma membrane K^+ transporter. Plant Physiol. 2008;148(2):796–807.
51. Shi H, Quintero FJ, Pardo JM, Zhu JK. The putative plasma membrane Na^+ /H^+ antiporter SOS1 controls long-distance Na^+ transport in plants. Plant Cell. 2002;14(2):465–477.
52. Luo M, Zhang Y, Chen K, Kong M, Song W, Lu B, Shi Y, Zhao Y, Zhao J. Mapping of quantitative trait loci for seedling salt tolerance in maize. Mol Breeding. 2019;39:64.
53. Luo M, Zhao Y, Zhang R, Xing J, Duan M, Li J, Wang N, Wang W, Zhang S, Chen Z, Zhang H, Shi Z, Song W, Zhao J. Mapping of a major QTL for salt tolerance of mature field-grown maize plants based on SNP markers. BMC Plant Biol. 2017;17(1):140.
54. Edgar RC. MUSCLE: a multiple sequence alignment method with reduced time and space complexity.BMC Bioinformatics. 2004;5:113.
55. Tamura K, Stecher G, Peterson D, Filipski A, Kumar S.MEGA6: molecular evolutionary genetics analysis version 6.0. Mol Biol Evol. 2013;30(12):2725–2729
56. Small I, Peeters N, Legeai F, Lurin C. Predotar: A tool for rapidly screening proteomes for N-terminal targeting sequences. Proteomics. 2004;4(6):1581–1590.
57. Emanuelsson O, Brunak S, von Heijne G, Nielsen H. Locating proteins in the cell using TargetP, SignalP and related tools. Nat Protoc. 2007;2(4):953–971.
58. Hu B, Jin J, Guo AY, Zhang H, Luo J, Gao G. GSDS 2.0: an upgraded gene feature visualization server. Bioinformatic. 2015;31:1296–1297.
59. Luo M, Zhao Y, Wang Y, Shi Z, Zhang P, Zhang Y, Song W, Zhao J. Comparative proteomics of contrasting maize genotypes provides insights into salt-stress tolerance mechanisms. J Proteome Res. 2018;17(1):141–153.
60. Dash S, Van Hemert J, Hong L, Wise RP, Dickerson JA. PLEXdb: gene expression resources for plants and plant pathogens. Nucleic Acids Res. 2010; 40(Database issue):D1194-1201.
61. Thomas S, Kenneth D, Livak J. Analyzing real-time PCR data by comparative CT method. Nat Protoc. 2008;3(6):1101–1108.
62. Lescot M. PlantCARE, a database of plant cis-acting regulatory elements and a portal to tools for in silico analysis of promoter sequences. Nucleic Acids Res. 2002;30(1):325–327.
63. Ren J, Wen L, Gao X, Jin C, Xue Y, Yao X. DOG 1.0: illustrator of protein domain structures.

Cell Res. 2009;19(2):271–273.

64. Yoo SD, Cho YH, Sheen J. *Arabidopsis* mesophyll protoplasts: a versatile cell system for transient gene expression analysis. Nat Protoc.2007;2(7):1565-1572.

65. Rodríguez-Navarro A, Ramos J. Dual system for potassium transport in *Saccharomyces cerevisiae*. J Bacteriol. 1984;159(3):940–945.

Figure Legends

Figure 1. Gene structures of *ZmCPA* genes.

The schematic diagram of the NJ tree of maize CPA genes at left was drawn based on Fig. 3. The exon-intron organization of *ZmCPA* genes (right) was analyzed by aligning the DNA and cDNA sequences of one *CPA* gene within GSDS 2.0 server (http://gsds.gao-lab.org/index.php). Introns and exons are shown as thin lines and yellow boxes, respectively. Numbers 0, 1 and 2 represent the different intron phases. Blue boxes at 5′ and 3′ ends represent untranslated regions (UTRs).

Figure 2. Phylogenetic tree of the *CPA* genes of maize, *Arabidopsis* and rice.

The NJ tree was constructed using MEGA 6.0 based on alignment of a total of 103 CPA proteins including 35 ZmCPAs, 42 AtCPAs and 26 OsCPAs. NHX, KEA and CHX subfamilies are divided into three (N1, N2 and N3), three (C1, C2, C3and C4) and two (K1 and K2) groups, respectively.

Figure 3. Phylogenetic tree of *ZmCPA* genes.

All of 35 ZmCPA proteins were aligned by the MUSCLE v3.8.31 program [54] and the alinment was used to construct the NJ tree with MEGA 6.0 [55]. *ZmCPA* genes are divided into three subfamlies, *ZmNHXs, ZmKEAs* and *ZmCHXs*.

Figure 4. Subcellular localization of ZmCHX16 and ZmNHX8 proteins.

The ZmCHX16-GFP (the upper panel) and ZmNHX8-GFP (the lower panel) fusion proteins were transiently expressed in maize protoplast cells co-transformed with the OsSCAMP1-RFP fusion construct as a membrane protein marker. The GFP and RFP signals were detected by Leica SP8 confocal fluorescent microscopy. Scale bar = 5μm.

Figure 5. Gene expression profile of *ZmCPA* genes in different tissues.

The normalized microarray expression data of *ZmCPA* genes was download from PLEXdb (http://www.plexdb.org/). Cluster analysis and the heatmap production was performed using Lianchuan BioCloud Platform (https://www.lc-bio.cn/overview).

Figure 6. Expression analysis of *ZmCPA* genes in the eight different tissues of B73 inbred line by semiq-RT-PCR.

The total RNA of eight tissues including seedling roots, seedling leaves, 5-cm immature ears, tassels, anthers, pollen, silk and whole seeds (20 days after pollination, DAP), were isolated and used to perform the semiq-RT-PCR of *ZmCPA* genes with the primers shown in Table S. The maize *Actin1* gene was an internal control.

Figure 7. Expression analysis of *ZmCPA* genes under salt stress conditions by qRT-PCR.

Expression analysis of *ZmCPA* genes under 100 mM NaCl or 100 mM KCl was carried out by quantitative reverse transcription-polymerase chain reaction (qRT-PCR). The y-axis represents the relative expression levels of *ZmCPA* genes compared with that of *actin1*. The x-axis represents different time points after salt treatment in each group. Error bars represent standard deviations for three replicates. qRT-PCR data were analyzed using the $2^{-\triangle\triangle Ct}$ method as described previously [65].

Figure 8. *ZmCPA* genes facilitate growth of yeast mutant strain AXT3K under salt stress.

The full length CDS sequences of *ZmNHX8*, *ZmCHX8*, *ZmCHX12*, *ZmCHX14*, *ZmCHX16*, *ZmKEA6* were cloned into the PDR196 vector, and then transformed into the yeast strain AXT3K (*ena1-4::HIS3,nha1::LEU2, nhx1::KanMX*). The yeast transformant cells cultured overnight were normalized in water to A_{600} of 0.8. Aliquos (5 μL) of 10-fold serial dilutions were spotted on AP plates supplemented with 20 mM NaCl at pH 7.5 (right panel) and normal AP plates as a control (left panel). The strains were grown at 29°C for 5 days and were photographed.

Figure 9. Growth performance of *zmnhx8* and *zmkea6* mutant seedlings under salt stress.

The point mutation sites of the EMS mutants *zmnhx8* and *zmkea6* were identified by PCR sequencing with the primers shown in Table S7. (a) The stop codons induced by EMS resulted in truncated proteins. Growth status (b), seedling length and dry weight (c) of the mutant seedlings under 100 mM NaCl treatment for 4 days were measured (n = 6, means ± SEM). Significant difference was calculated using Student's t-test. * indicants p-value < 0.05.

Table 1. Information of maize *CPA* genes identified in this study.

Gene Name	Gene Model	Chromosomal Location	CDS (bp)	Protein Length (aa)
ZmNHX1	*Zm00001d028330*	Chr1: 31041489-31049951	1599	532
ZmNHX2	*Zm00001d031232*	Chr1: 182925112-182945175	3411	1136
ZmNHX3	*Zm00001d003728*	Chr2: 56632216-56643296	2367	788
ZmNHX4	*Zm00001d048732*	Chr4: 4469601-4475393	1641	546
ZmNHX5	*Zm00001d019978*	Chr7: 81486383-81509317	1611	536
ZmNHX6	*Zm00001d020892*	Chr7: 135679272-135687679	1491	496
ZmNHX7	*Zm00001d021844*	Chr7: 164344371-164361391	2820	939
ZmNHX8	*Zm00001d022504*	Chr7: 179047417-179052457	1620	539
ZmNHX9	*Zm00001d045883*	Chr9: 45473833-45477106	1638	545
ZmNHX10	*Zm00001d048459*	Chr9: 156705048-156709982	1440	479
ZmNHX11	*Zm00001d024832*	Chr10: 90134129-90141743	1680	559
ZmNHX12	*Zm00001d025052*	Chr10: 101802712-101807654	1563	520
ZmNHX13	*Zm00001d026118*	Chr10: 138832710-138862665	2115	704
ZmCHX1	*Zm00001d031077*	Chr1: 176192733-176196049	2388	795
ZmCHX2	*Zm00001d031078*	Chr1: 176200721-176205899	2061	686
ZmCHX3	*Zm00001d005032*	Chr2: 155039785-155042337	2553	850
ZmCHX4	*Zm00001d041198*	Chr3: 105028259-105030854	2529	842
ZmCHX5	*Zm00001d044623*	Chr3: 233503244-233505658	2415	804
ZmCHX6	*Zm00001d049663*	Chr4: 39074035-39076527	2493	830
ZmCHX7	*Zm00001d050509*	Chr4: 94925858-94928987	2232	743
ZmCHX8	*Zm00001d053237*	Chr4: 221575337-221578465	2478	825
ZmCHX9	*Zm00001d017805*	Chr5:207302222-207308368	2484	827
ZmCHX10	*Zm00001d035631*	Chr6:37793506-37814621	2571	856
ZmCHX11	*Zm00001d038517*	Chr6:159098609-159101687	2598	865
ZmCHX12	*Zm00001d021461*	Chr7:152741608-152744549	2424	807
ZmCHX13	*Zm00001d009889*	Chr8:87464523-87467367	2391	796
ZmCHX14	*Zm00001d010601*	Chr8:121526743-121529490	2475	824
ZmCHX15	*Zm00001d010629*	Chr8:122278283-122281316	2874	957
ZmCHX16	*Zm00001d012521*	Chr8:176021482-176024817	2628	875
ZmKEA1	*Zm00001d027466*	Chr1:5893819-5906194	1791	596
ZmKEA2	*Zm00001d001788*	Chr2:935639-948444	3480	1159
ZmKEA3	*Zm00001d041308*	Chr3:111434917-111440097	2397	798
ZmKEA4	*Zm00001d036981*	Chr6:108202268-108211871	1848	615
ZmKEA5	*Zm00001d046231*	Chr9:73621310-73635421	1872	623
ZmKEA6	*Zm00001d026645*	Chr10:149326566-149340249	3315	1104

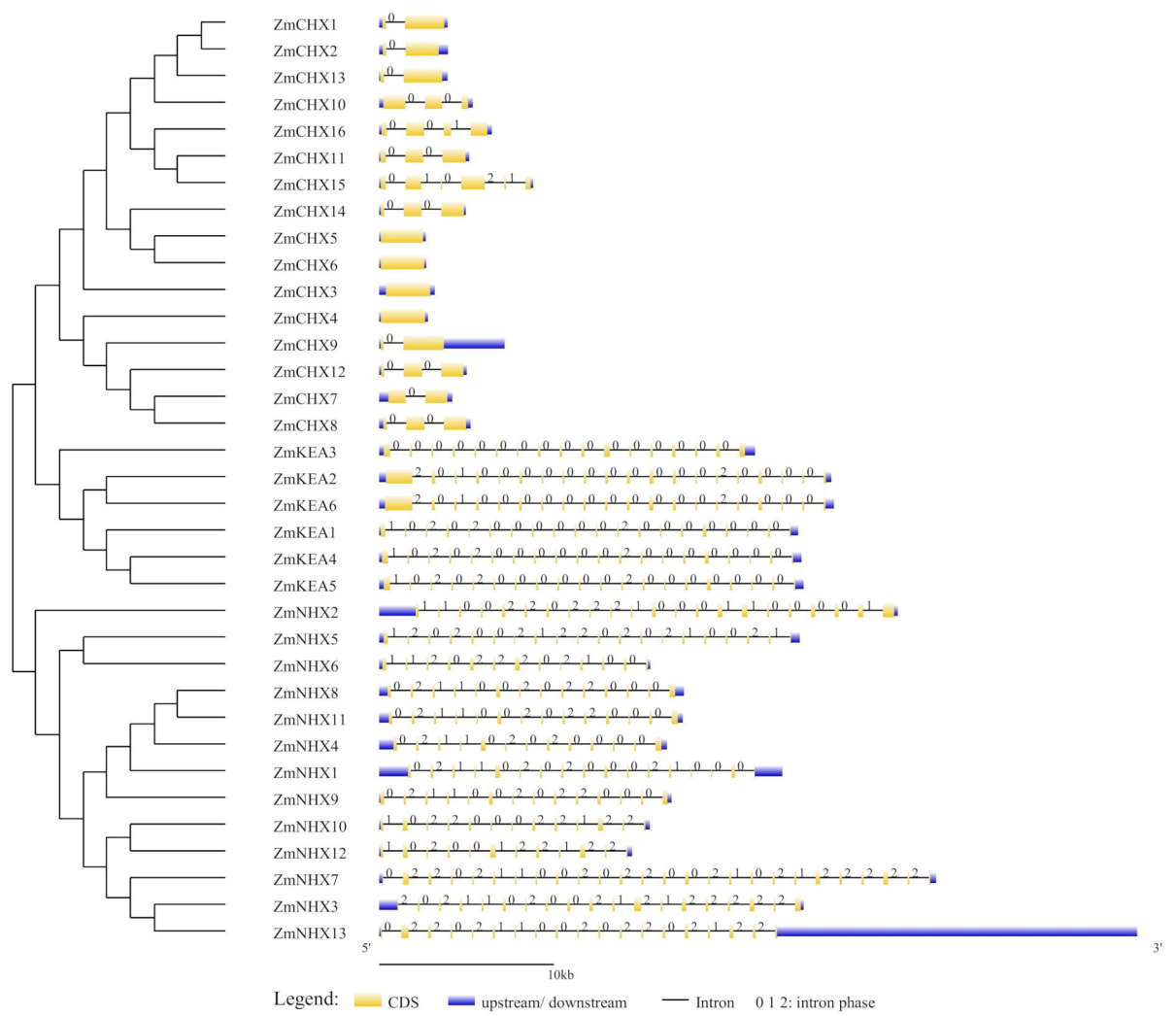
ZmCHX1
ZmCHX2
ZmCHX13
ZmCHX10
ZmCHX16
ZmCHX11
ZmCHX15
ZmCHX14
ZmCHX5
ZmCHX6
ZmCHX3
ZmCHX4
ZmCHX9
ZmCHX12
ZmCHX7
ZmCHX8
ZmKEA3
ZmKEA2
ZmKEA6
ZmKEA1
ZmKEA4
ZmKEA5
ZmNHX2
ZmNHX5
ZmNHX6
ZmNHX8
ZmNHX11
ZmNHX4
ZmNHX1
ZmNHX9
ZmNHX10
ZmNHX12
ZmNHX7
ZmNHX3
ZmNHX13
5'
3'
10kb
Legend:
CDS
upstream/ downstream
Intron
0 1 2: intron phase

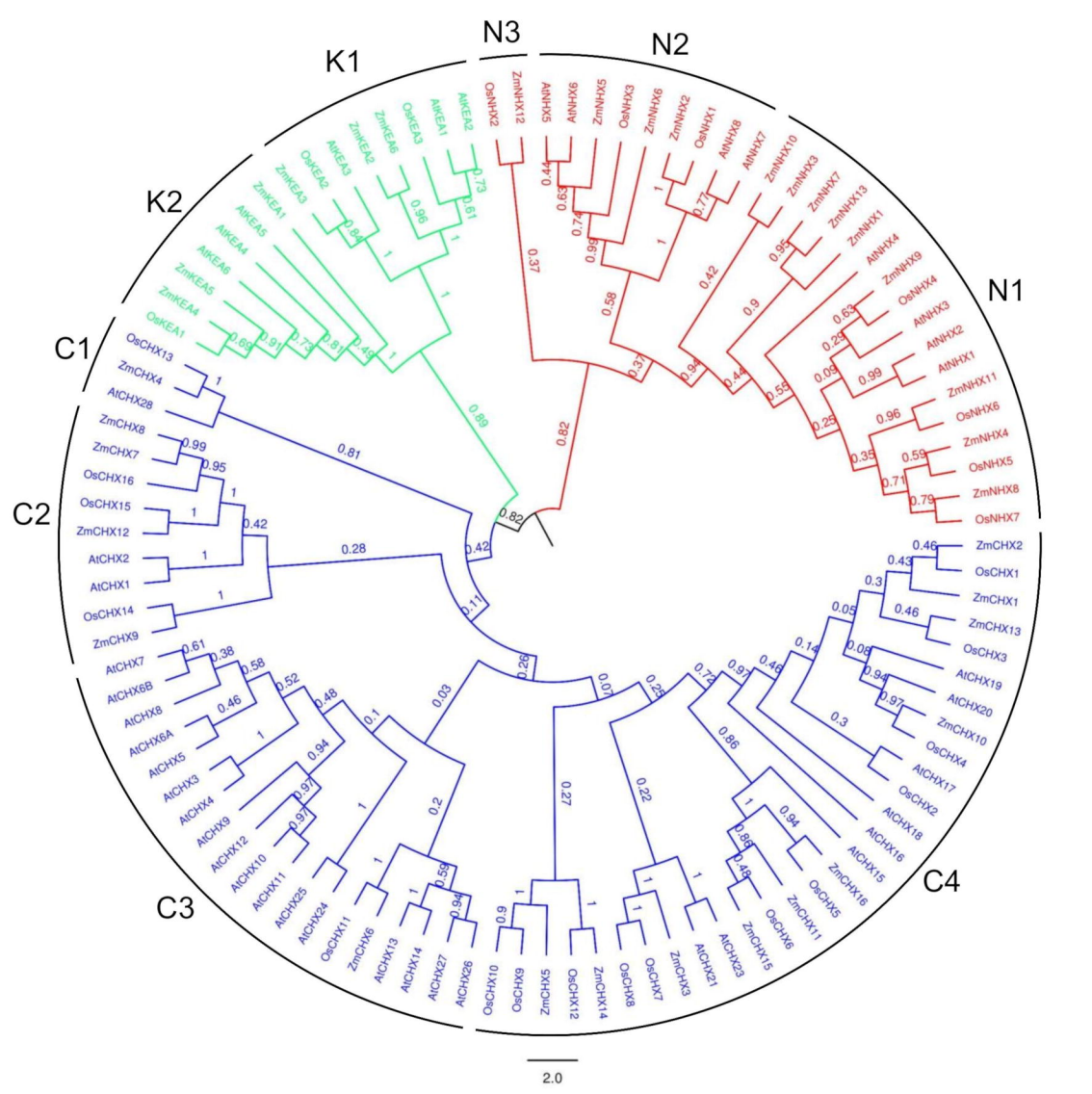
N3
N2
K1
K2
N1
C1
C2
C3
C4
ZmNHX12
AtNHX5
AtNHX9
ZmNHX5
OsNHX3
ZmNHX6
ZmNHX2
OsNHX1
AtNHX8
AtNHX7
ZmNHX10
ZmNHX3
ZmNHX7
ZmNHX13
ZmNHX1
AtNHX4
ZmNHX9
OsNHX4
AtNHX3
AtNHX2
AtNHX1
ZmNHX11
OsNHX6
ZmNHX4
OsNHX5
ZmNHX8
OsNHX7
OsNHX2
AtKEA1
AtKEA2
OsKEA3
ZmKEA6
ZmKEA2
AtKEA3
OsKEA2
ZmKEA3
ZmKEA1
AtKEA5
AtKEA4
AtKEA6
ZmKEA5
ZmKEA4
OsKEA1
OsCHX13
ZmCHX4
AtCHX28
ZmCHX8
ZmCHX7
OsCHX16
OsCHX15
ZmCHX12
AtCHX2
AtCHX1
OsCHX14
ZmCHX9
AtCHX7
AtCHX6B
AtCHX8
AtCHX6A
AtCHX5
AtCHX3
AtCHX4
AtCHX9
AtCHX12
AtCHX10
AtCHX11
AtCHX25
AtCHX24
OsCHX11
ZmCHX6
AtCHX13
AtCHX14
AtCHX27
AtCHX26
OsCHX10
OsCHX9
ZmCHX5
OsCHX12
ZmCHX14
OsCHX8
OsCHX7
ZmCHX3
AtCHX21
AtCHX23
ZmCHX15
OsCHX6
OsCHX5
ZmCHX11
ZmCHX16
AtCHX15
AtCHX16
AtCHX18
OsCHX2
AtCHX17
OsCHX4
ZmCHX10
AtCHX20
AtCHX19
OsCHX3
ZmCHX13
ZmCHX1
OsCHX1
ZmCHX2
2.0

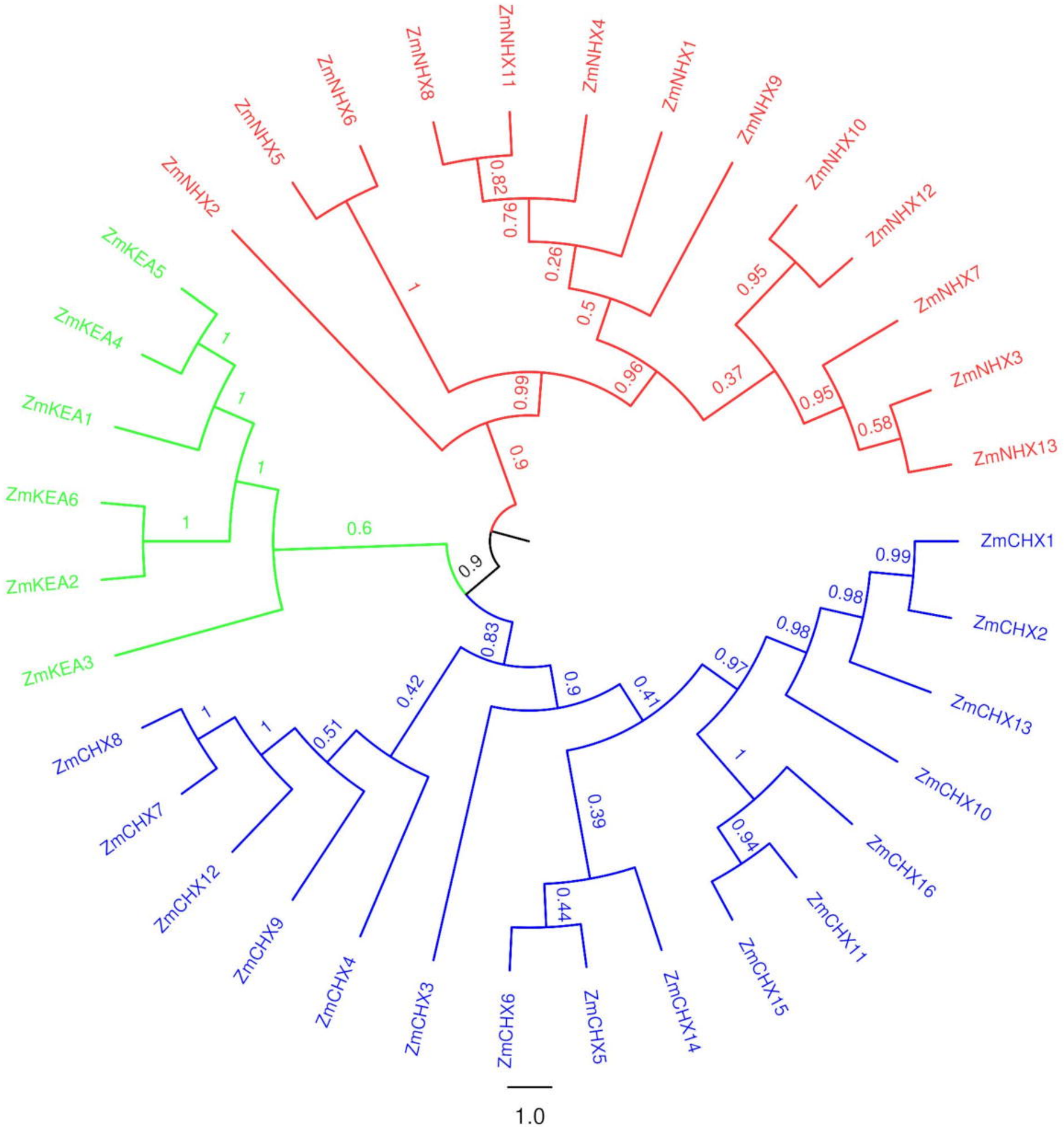
ZmNHX11
ZmNHX8
ZmNHX4
ZmNHX1
ZmNHX9
ZmNHX10
ZmNHX12
ZmNHX7
ZmNHX3
ZmNHX13
ZmNHX6
ZmNHX5
ZmNHX2
ZmKEA5
ZmKEA4
ZmKEA1
ZmKEA6
ZmKEA2
ZmKEA3
ZmCHX1
ZmCHX2
ZmCHX13
ZmCHX10
ZmCHX16
ZmCHX11
ZmCHX15
ZmCHX14
ZmCHX5
ZmCHX6
ZmCHX3
ZmCHX4
ZmCHX9
ZmCHX12
ZmCHX7
ZmCHX8
0.82
0.76
0.26
0.5
0.95
0.37
0.96
0.99
1
0.9
0.6
0.9
0.83
0.42
0.51
1
1
0.9
0.41
0.39
0.44
0.97
0.98
0.98
0.99
1
0.94
1
1
1
1
1
1.0

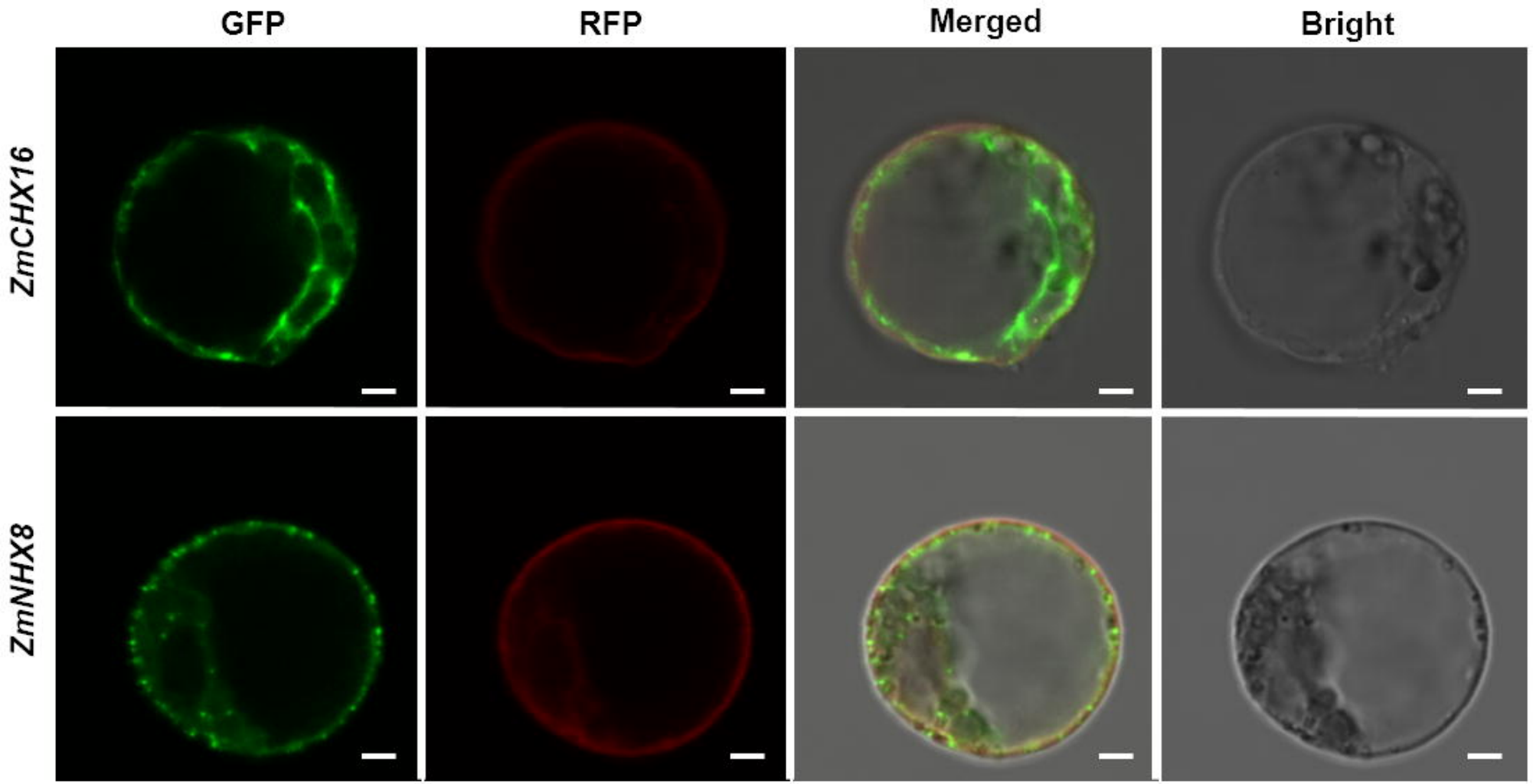
GFP
RFP
Merged
Bright
ZmCHX16
ZmNHX8

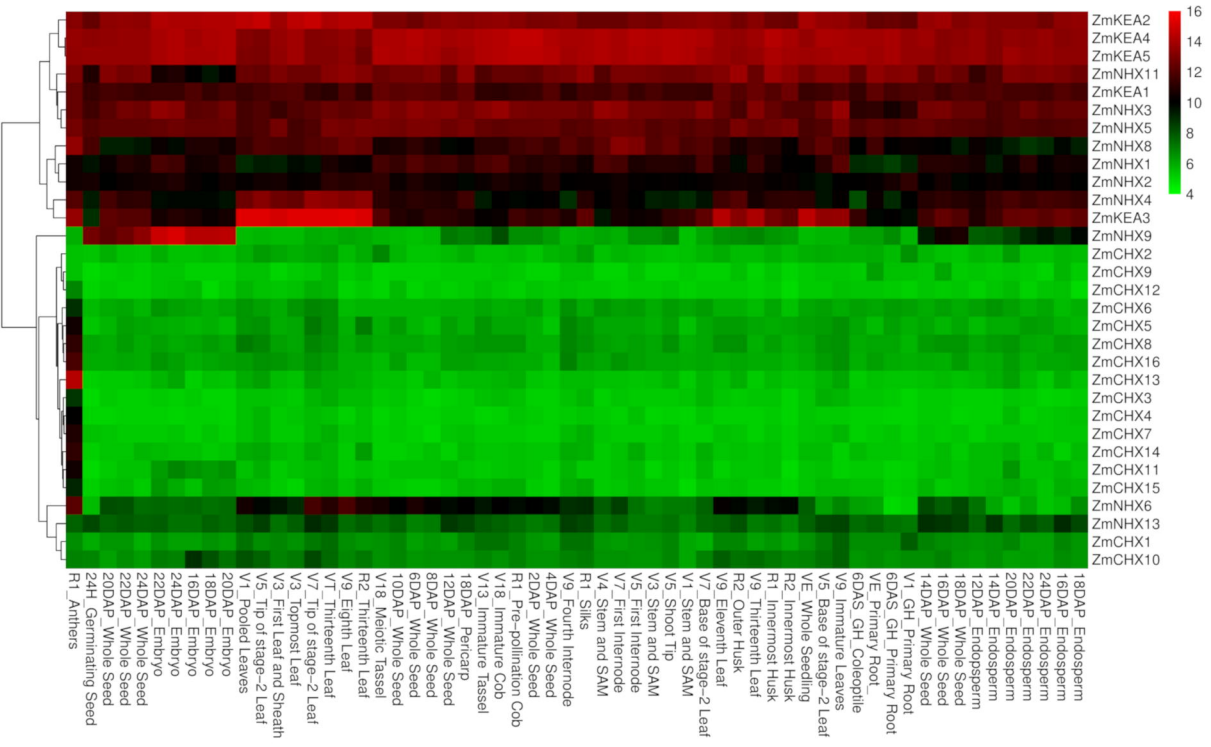
16
14
12
10
8
6
4
ZmKEA2
ZmKEA4
ZmKEA5
ZmNHX11
ZmKEA1
ZmNHX3
ZmNHX5
ZmNHX8
ZmNHX1
ZmNHX2
ZmNHX4
ZmKEA3
ZmNHX9
ZmCHX2
ZmCHX9
ZmCHX12
ZmCHX6
ZmCHX5
ZmCHX8
ZmCHX16
ZmCHX13
ZmCHX3
ZmCHX4
ZmCHX7
ZmCHX14
ZmCHX11
ZmCHX15
ZmNHX6
ZmNHX13
ZmCHX1
ZmCHX10
18DAP_Endosperm
16DAP_Endosperm
24DAP_Endosperm
22DAP_Endosperm
20DAP_Endosperm
14DAP_Endosperm
12DAP_Endosperm
18DAP_Whole Seed
16DAP_Whole Seed
14DAP_Whole Seed
1V1_GH_Primary Root
6DAS_GH_Primary Root
VE_Primary Root
6DAS_GH_Coleoptile
V5_Base of stage-2 Leaf
V9_Immature Leaves
VE_Whole Seedling
R1_Innermost Husk
R2_Innermost Husk
V9_Thirteenth Leaf
R2_Outer Husk
V9_Eleventh Leaf
V7_Base of stage-2 Leaf
V1_Stem and SAM
V5_Shoot Tip
V3_Stem and SAM
V5_First Internode
V7_First Internode
V4_Stem and SAM
R1_Silks
V9_Fourth Internode
4DAP_Whole Seed
2DAP_Whole Seed
R1_Pre-pollination Cob
V18_Immature Cob
V13_Immature Tassel
18DAP_Pericarp
12DAP_Whole Seed
8DAP_Whole Seed
6DAP_Whole Seed
10DAP_Whole Seed
V18_Meiotic Tassel
R2_Thirteenth Leaf
V9_Eighth Leaf
V7_Thirteenth Leaf
V7_Tip of stage-2 Leaf
V2_Topmost Leaf
V3_First Leaf and Sheath
V5_Tip of stage-2 Leaf
V1_Pooled Leaves
20DAP_Embryo
18DAP_Embryo
16DAP_Embryo
24DAP_Embryo
22DAP_Embryo
24DAP_Whole Seed
22DAP_Whole Seed
20DAP_Whole Seed
24H_Germinating Seed
R1_Anthers

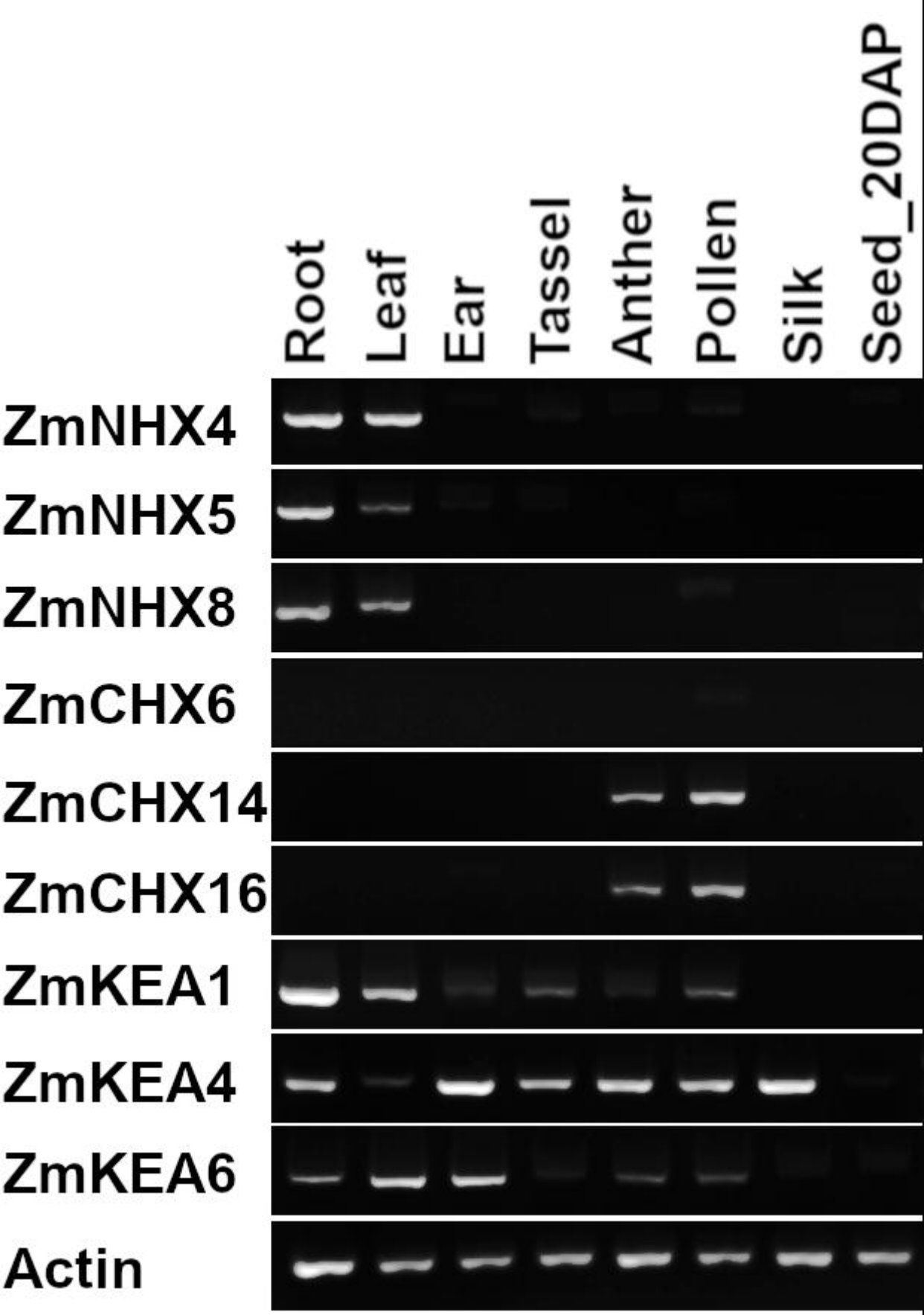
Root
Leaf
Ear
Tassel
Anther
Pollen
Silk
Seed_20DAP
ZmNHX4
ZmNHX5
ZmNHX8
ZmCHX6
ZmCHX14
ZmCHX16
ZmKEA1
ZmKEA4
ZmKEA6
Actin

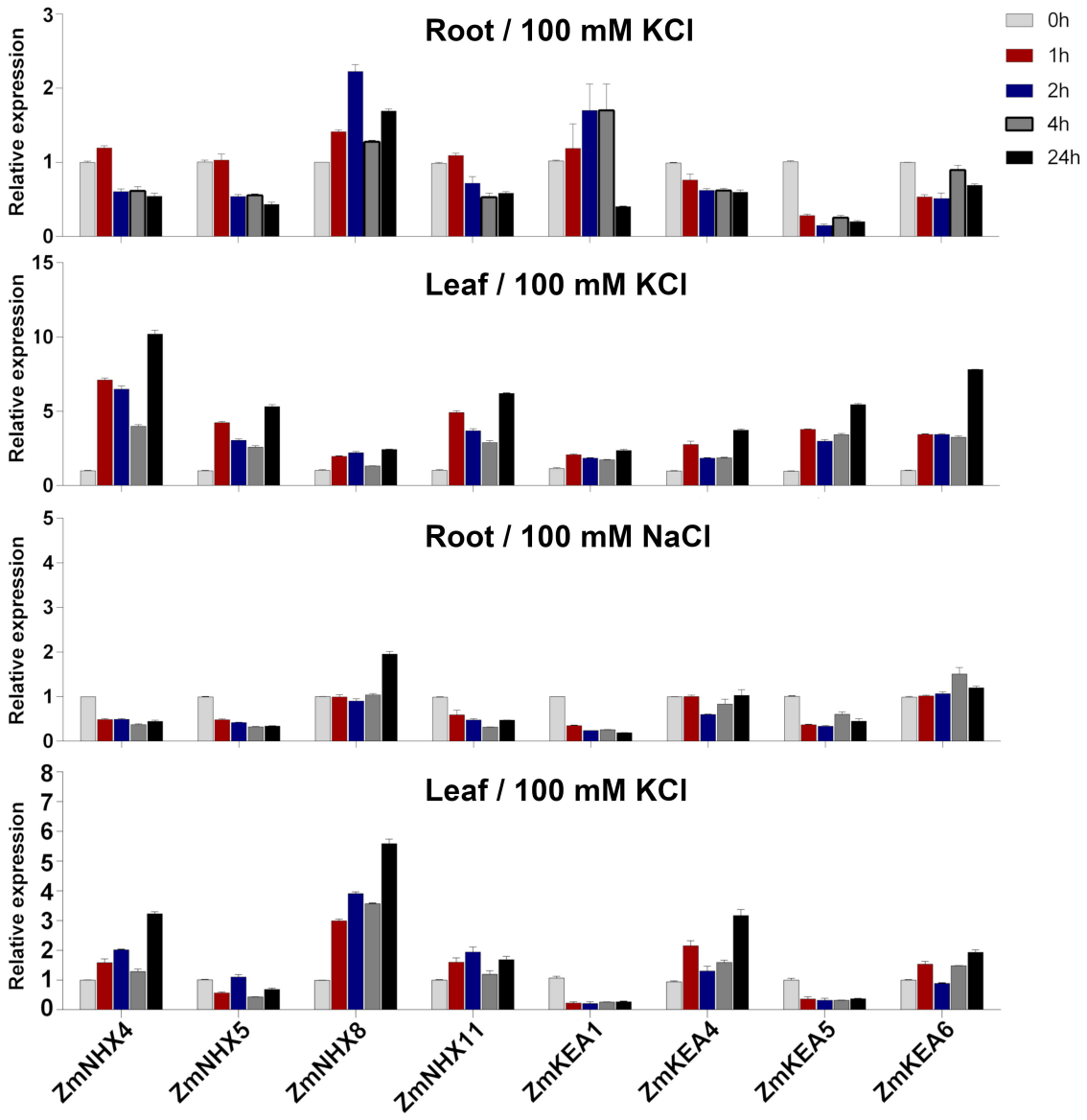
Root / 100 mM KCl
Leaf / 100 mM KCl
Root / 100 mM NaCl
Leaf / 100 mM KCl
Relative expression
0h
1h
2h
4h
24h
ZmNHX4
ZmNHX5
ZmNHX8
ZmNHX11
ZmKEA1
ZmKEA4
ZmKEA5
ZmKEA6

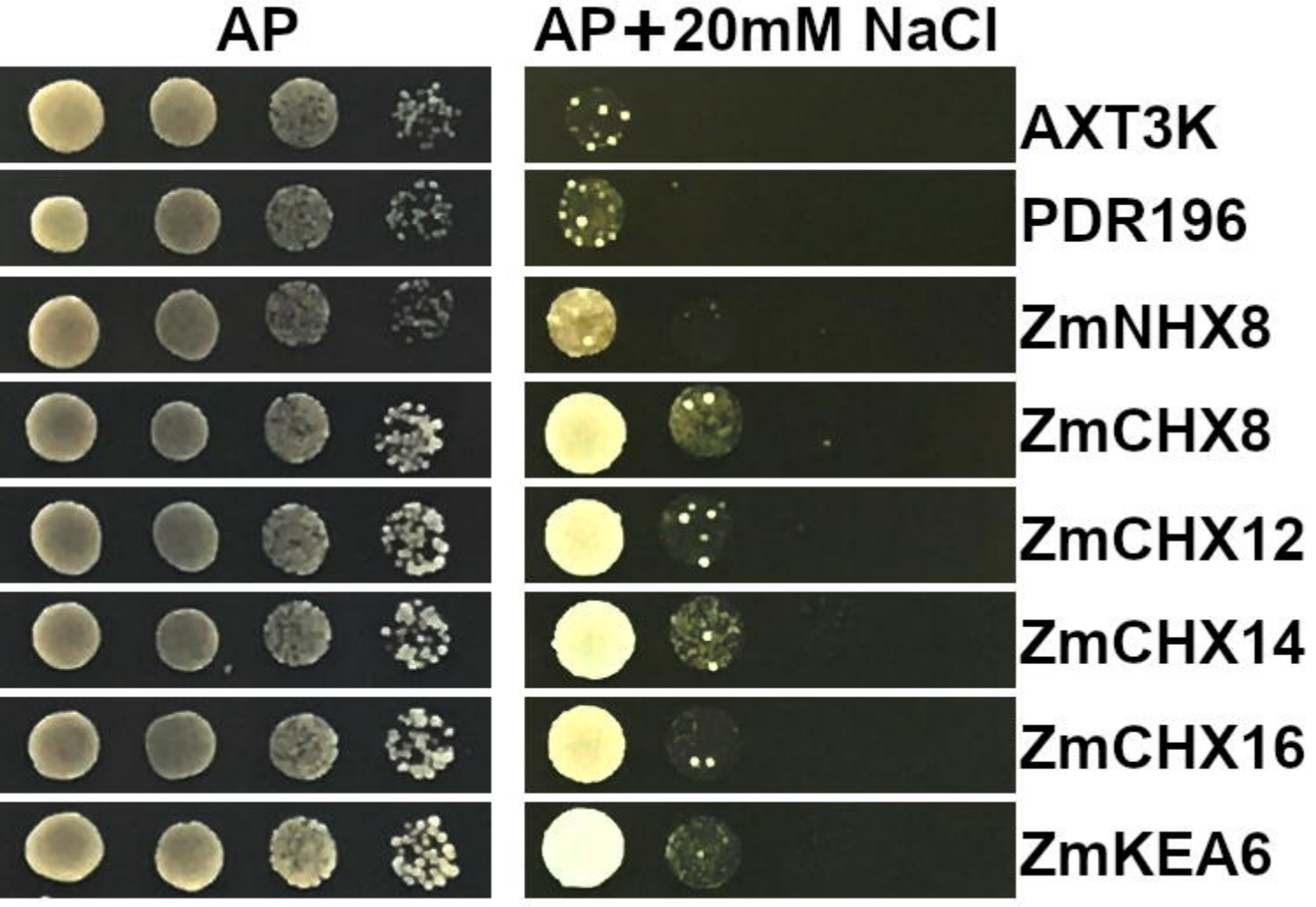
AP
AP+20mM NaCl
AXT3K
PDR196
ZmNHX8
ZmCHX8
ZmCHX12
ZmCHX14
ZmCHX16
ZmKEA6

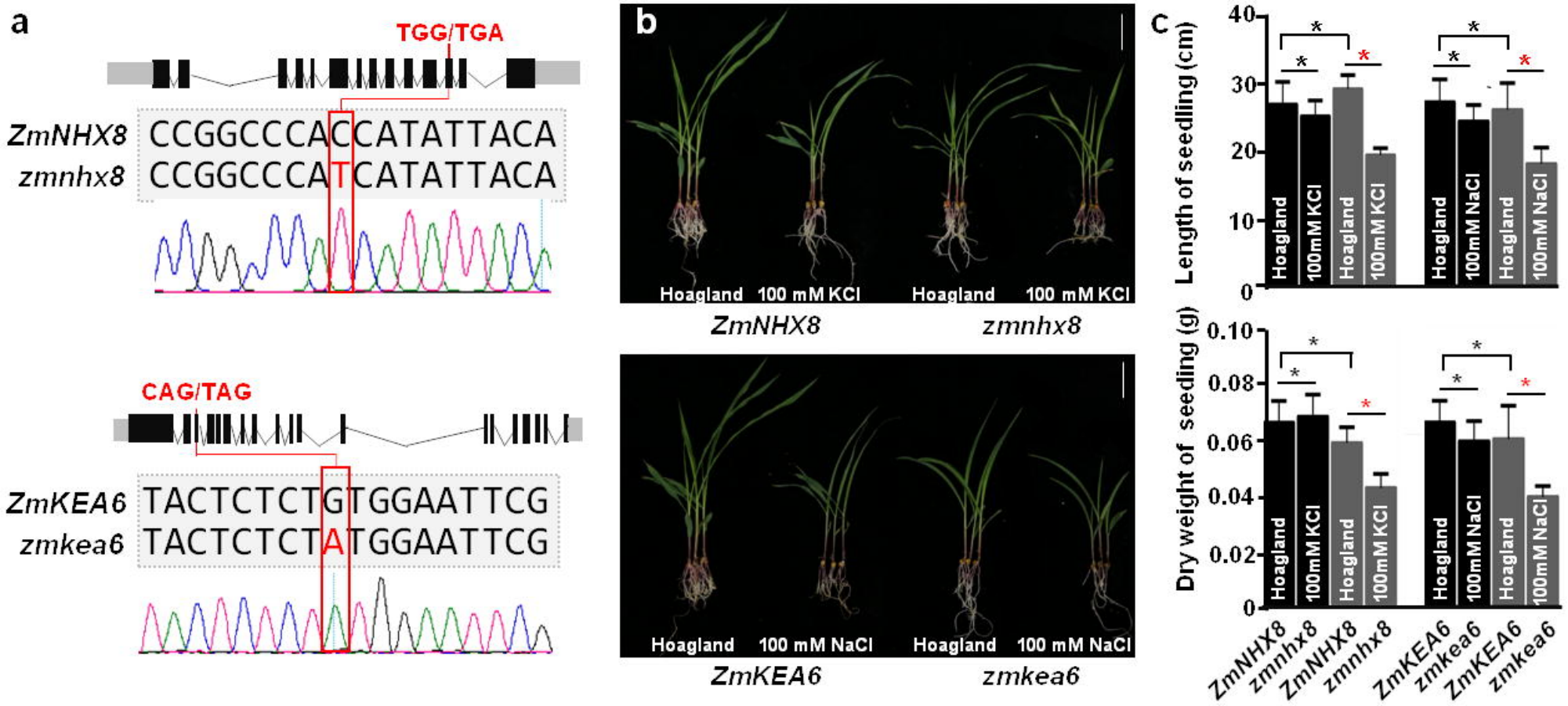
a
TGG/TGA
ZmNHX8 CCGGCCCACCATATTACA
zmnhx8 CCGGCCCATCATATTACA
CAG/TAG
ZmKEA6 TACTCTCTGTGGAATTCG
zmkea6 TACTCTCTATGGAATTCG
b
Hoagland 100 mM KCl
Hoagland 100 mM KCl
ZmNHX8
zmnhx8
Hoagland 100 mM NaCl
Hoagland 100 mM NaCl
ZmKEA6
zmkea6
c
Length of seedling (cm)
Dry weight of seedling (g)
Hoagland
100mM KCl
100mM NaCl
ZmNHX8
zmnhx8
ZmKEA6
zmkea6